



Quantitative comparison between the effective energy utilization efficiency of triboelectric nanogenerator and electromagnetic generator post power management

Chaosheng Hu^{a,b}, Ya Yang^{a,b,c,*}, Zhong Lin Wang^{a,b,d,*}

^a CAS Center for Excellence in Nanoscience, Beijing Key Laboratory of Micro-nano Energy and Sensor, Beijing Institute of Nanoenergy and Nanosystems, Chinese Academy of Sciences, Beijing 101400, PR China

^b School of Nanoscience and Technology, University of Chinese Academy of Sciences, Beijing 100049, PR China

^c Center on Nanoenergy Research, School of Physical Science and Technology, Guangxi University, Nanning 530004, PR China

^d School of Material Science and Engineering, Georgia Institute of Technology, Atlanta, GA 30332-0245, USA

ARTICLE INFO

Keywords:

Triboelectric nanogenerator
Electromagnetic generator
Rectification
Frequency
Energy utilization efficiency

ABSTRACT

Triboelectric nanogenerator (TENG) is an energy technology that produces an output of high voltage but low current, and its output power is proportional to operation frequency (f). While the electromagnetic generator (EMG) gives an output of high current but low voltage, and its output power is proportional f^2 . Since both TENG and EMG gives an alternating current (AC), which has to be rectified into direct current (DC) for practical use. With considering the different degree of voltage and power losses at the rectification circuit owing to the threshold operation voltage of a diode, this is the first quantitative comparison between the effective energy utilization efficiency of TENG and EMG. The results demonstrate that the frequency range in which the maximum peak power of TENG outperforms EMG is expanded after rectification due to the more severe power loss of EMG than that of TENG. Besides, the average power loss rate of TENG is consistently lower than that of EMG, and it is especially obvious at low frequencies. Moreover, the energy utilization efficiency of TENG is always superior to that of EMG after rectification, with a maximum of 98.84 % for TENG while only 66.36 % for EMG. This study reveals that the loss caused by the rectification circuit of TENG is much lower than that of EMG, which lays a solid foundation for the applications of DC-TENG.

1. Introduction

With the rapid development of the Internet of Things and artificial intelligence, there is an urgent need for sustainable, environmentally friendly, and widely distributed energy sources. As a new energy harvesting technology, triboelectric nanogenerator (TENG) can effectively scavenge mechanical energy from the environment [1–6], and can be applied to self-powered sensors [7–11], micro/nano systems [12,13] and blue energy [14–16]. Due to the advantages of low-cost, environmental benign, a wide range of material choices and high open circuit voltage [17,18], TENGs have become increasingly popular among researchers. Meanwhile, electromagnetic generator (EMG) has long been an indispensable part of people's life as a classical energy supply technology. In order to maximize energy utilization, the hybrid TENG-EMG has been reported for harvesting the mechanical energy such as wind

[19–21], vibration [22–24], and rotational energy [25,26]. However, the conventional TENG based on triboelectric effects and electrostatic induction and EMG based on the law of electromagnetic induction gives an alternating current (AC). A rectification circuit is needed to convert the AC into direct current (DC) in order to be effectively utilized for driving electronics.

In recent years, many methods have been explored to achieve DC TENG [27–31], such as designing specific structures to realize phase coupling [32], achieving air breakdown via dielectric breakdown effect [33–37], and selecting semiconductors as tribo-materials to enable unidirectional flow of charge [38]. However, all these methods impose certain special requirements on the generators, such as the delicate design of the structures, high charge density, and special material properties, which limit the universality of the application of the method. The integration of a management circuit as one of the common methods

* Corresponding authors at: CAS Center for Excellence in Nanoscience, Beijing Key Laboratory of Micro-nano Energy and Sensor, Beijing Institute of Nanoenergy and Nanosystems, Chinese Academy of Sciences, Beijing 101400, PR China.

E-mail addresses: yayang@binn.cas.cn (Y. Yang), zhong.wang@mse.gatech.edu (Z.L. Wang).

<https://doi.org/10.1016/j.nanoen.2022.107760>

Received 6 August 2022; Received in revised form 27 August 2022; Accepted 29 August 2022

Available online 1 September 2022

2211-2855/© 2022 Elsevier Ltd. All rights reserved.

to achieve DC for TENG [39], which is also applicable to EMG. In addition, the introduction of these circuit elements can have a relatively positive impact on the output results, but it is worth noting that the electronics also consume a certain amount of energy in the circuit, and the more electronics will consume more energy. Therefore, using the simplest circuit structure with only one rectifier to directly compare the energy loss of TENG and EMG in the same circuit can avoid the problem of different energy loss due to the connection of different management circuits. Previous reports have systematically investigated the differences between TENGs and EMGs in terms of theoretical models, operating mechanisms and output equations for energy harvesting, and found a high degree of similarity and symmetry with each other [40], and have also focused on comparing the energy harvesting capabilities of TENG and EMG at low frequency [41] and small-amplitude [42]. And some studies increase the output energy by reducing the internal resistance of the TENG [43–45]. But these studies use the as-output AC signal without rectification and there is a lack of systematic studies on the energy loss of both generators in conversion from AC to DC.

In this work, we fabricated a TENG and an EMG in contact-separation mode to systematically compare the energy loss of both types of generators in obtaining DC output through rectifier bridge. To avoid the problem of different energy loss due to the tilt of the cutting magnetic induction line direction, the magnet is moving vertically directly above the copper coil to ensure the maximum change of magnetic flux during the motion. The peak output powers of the two types of generators connected with matched resistors were compared at different frequencies and demonstrated that the performance of TENG was superior to that of EMG at low frequencies and the loss rate of the rectified EMG was much severe than that of the TENG. In addition, the loss rate of average power and energy of EMG are more severe than that of TENG after rectification. Moreover, as the frequency increases, the energy utilization efficiency via rectifier module of both TENG and EMG becomes higher, and that of TENG is consistently superior to that of EMG at various frequencies. Also, this contrasting characteristics is verified in EMG with different number of turns and different wire diameters. This work highlights the impact of rectifier circuit on energy utilization and demonstrates the lower power and energy losses of TENG compared to EMG during the conversion of AC to DC. In addition, it provides a very important reference value for the applications of TENG in driving electronic devices with high efficiency in DC power supplies.

2. Experimental section

2.1. Fabrication of EMG and TENG

EMG is mainly composed of two parts, a cylindrical magnet and a coil of the same size encapsulated in acrylic plate, where the magnet and coil have a diameter of 30 mm and a thickness of 5 mm. For the magnet part, a rectangular acrylic plate with a thickness of 5 mm, a length of 33 mm and a chamfer radius of 6 mm is manufactured by a laser cutting machine of PLS 4.75, and a hole with a diameter of 30 mm is dug in the middle to place the magnet. Then two 1 mm rectangular acrylic plates with 33 mm length and 6 mm chamfer radius were manufactured and pasted on the front and back of the magnet to complete the package. The size of the acrylic plates used to encapsulate the copper coils is the same as above. The wire diameter and the number of turns of the coil is 0.05 mm and 13,000 T, and the resistance is 6.70 k Ω . In addition, for other coils with different wire diameter and different turns in the text, the encapsulation materials and methods are the same as above. The resistance of coils (13,000 T) with wire diameter of 0.06 mm, 0.07 mm, 0.08 mm, 0.1 mm are 4.43 k Ω , 3.25 k Ω , 2.49 k Ω , 1.54 k Ω , respectively, and coils (0.05 mm) with turns of 9000 T, 17,000 T, 21,000 T, 25,000 T are 4.49 k Ω , 8.57 k Ω , 10.45 k Ω , 12.34 k Ω , respectively.

TENG is made of an upper part and a lower part. The upper part is made of nylon film of 25 μm , aluminum foil of 20 μm and acrylic plate of 1 mm in sequence, all of which are shaped into a square with a 50 mm

length and a 6 mm radius chamfer. The lower part is made of 30 μm FEP, 20 μm aluminum foil, 3 mm sponge and 1 mm acrylic sheet of in order, and the size of the material is the same as that of the upper part. The horizontal dimensions of the prepared TENG is larger than that of the EMG is to keep the volumes of both generators essentially the same.

2.2. Control of contact and separation

The regulation of the frequency of the contact and separation process of the two generators is achieved by a linear motor of model H01-23 \times 86/160. The displacement of the motor is fixed at 10 mm, and the acceleration and deceleration are set to a sufficiently large value of 200 m/s² to ensure that the motion process can be approximated as uniform motion. One part of the generator is fixed to the linear motor to achieve the motion, and the other part is fixed to the M-37 multi-axis tilting platform to ensure that the two contact surfaces are parallel during contact.

2.3. Electrical measurements

The voltage and current of the generator were measured by KEITHLEY 6514 programmable electrometer. The model of the rectifier bridge in experiment is DF06, which is a commercially available electronic component.

3. Results and discussion

Fig. 1a shows the 3D schematic of the contact-separated EMG and TENG. The EMG consists of a cylindrical magnet and a copper coil, both of which are sandwiched in the middle by acrylic sheets. The TENG is composed of nylon film, fluorinated ethylene propylene (FEP) film, Al foil, sponge and acrylic plate. Nylon and FEP are used as tribo-layers, sponge is used as buffer layer to achieve full contact of Nylon and FEP, and acrylic plate is used as the substrate. The specific fabrication processes are described in detail in Section 2, and the specific working principle of the two generators are exhibited in Fig. S1 (Supporting information). Fig. 1b displays the cross-sectional view and the corresponding photographs of EMG (left) and TENG (right), respectively. Fig. 1c demonstrates the circuit diagrams of EMG and TENG without and with rectification. Before rectification, the load resistor is directly connected to the generator, and the output voltage, optimal power and energy of the load can be obtained by changing the resistance value. While the rectifier is connected, the output performance above is decreased due to the loss caused by the rectifier bridge. Fig. 1d compares the average power loss rate of EMG and TENG, which is calculated by the ratio of the average power loss caused by rectification and the average power before rectification, indicating that the loss rate decreases roughly with increasing frequency and the loss rate of TENG is consistently lower than that of EMG at the same frequency, reaching a maximum of 31.73 % for TENG and 99.74 % for EMG at the lowest frequency of 1.5 Hz. Besides, the average power loss rate of TENG is lowest at 5 Hz and that of EMG gradually decreases with increasing frequency, which may be related to the inadequate contact between the two tribo-materials of TENG at high frequency, and the corresponding explanation is described in detail in the Supplementary Note 2. Moreover, the energy loss rate of both types of generators is shown in Fig. 1e and demonstrates that the loss rate of TENG is always lower than that of EMG at various frequencies, and the loss rate is more severe at lower frequencies. Similarly, the energy loss rate can be calculated by the ratio of the lost energy caused by rectification to the energy before rectification. The results reveal that the loss of power and energy of EMG at the rectification circuit is more serious than that of TENG at various frequencies.

Fig. 2a compares the output voltages of the load before and after rectification with different load resistances connected at 1.5 Hz. The voltages are attenuated after rectification for both EMG and TENG, and

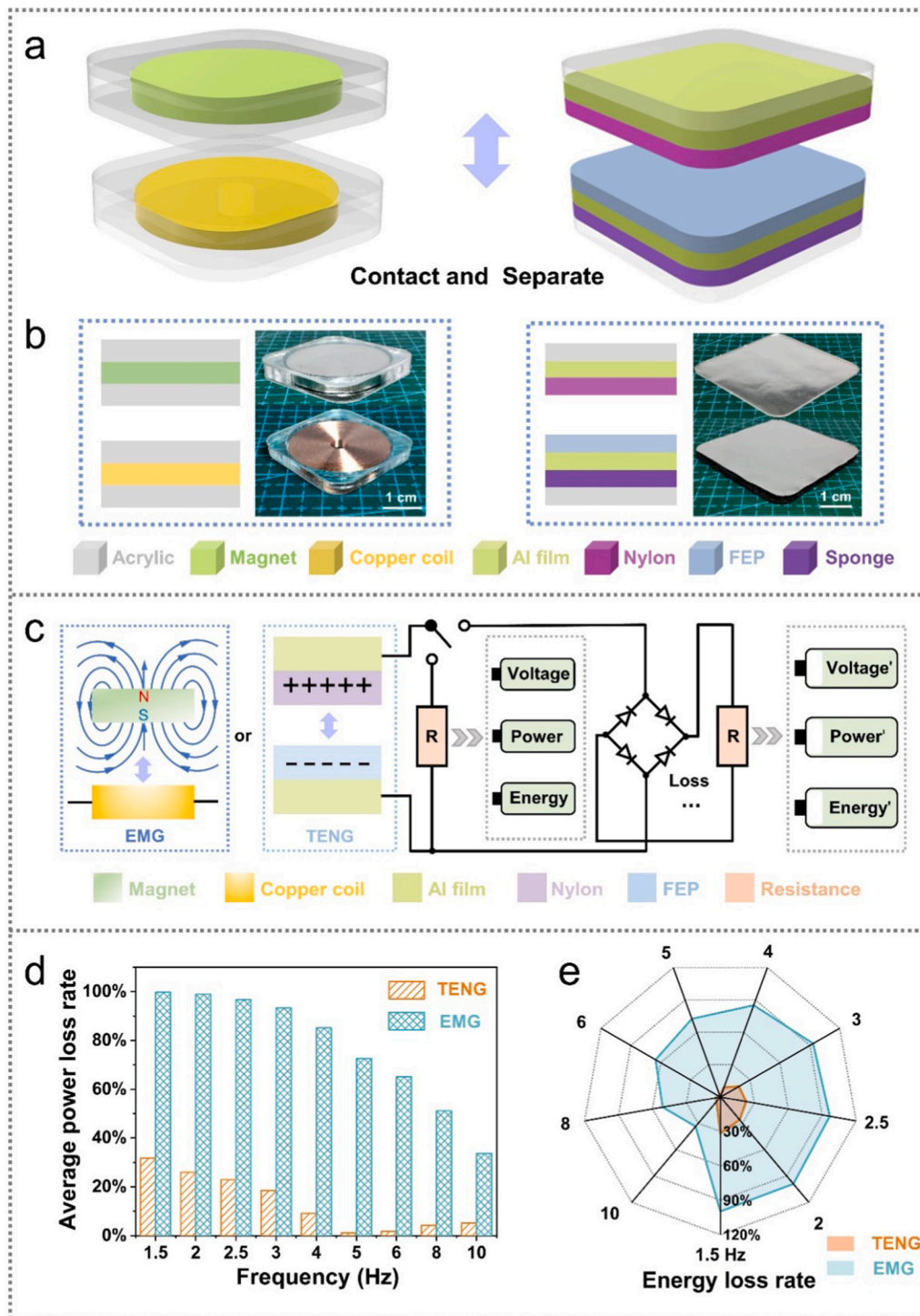


Fig. 1. Structure of EMG and TENG and corresponding circuit diagram before and after rectification. (a) Three-dimensional structure of EMG (left) and TENG (right). (b) Cross-sectional diagrams and photographs of EMG (left) and TENG (right). (c) Circuit diagrams of both generators before and after rectification. (d–e) Average power loss rate (d) and energy loss rate (e) of EMG and TENG at different frequencies after rectification.

it decreases greatly for EMG while insignificant for TENG. To understand the reason for the difference in voltage drop of the two generators after rectification, we analyze the loss rate of voltage of both generators with different external resistors connected theoretically according to the circuit diagram Fig. S1 (c) (Supporting information), which can be expressed as:

$$\eta_{V_{\text{loss}}} = \frac{V_{\text{Not rectified}} - V_{\text{Rectified}}}{V_{\text{Not rectified}}} = \frac{\frac{V_{\text{OC}} \cdot R_L}{R_L + r} - \frac{V_{\text{OC}} \cdot R_L}{R_L + r + R_R}}{\frac{V_{\text{OC}} \cdot R_L}{R_L + r}} = \frac{R_R}{R_L + r + R_R} \quad (1)$$

where $\eta_{V_{\text{loss}}}$ is the loss rate of voltage, $V_{\text{Not rectified}}$ and $V_{\text{Rectified}}$ are the voltage before and after rectification, respectively. Besides, r , R_L and R_R are the resistance of the generator, external load and the rectifier bridge,

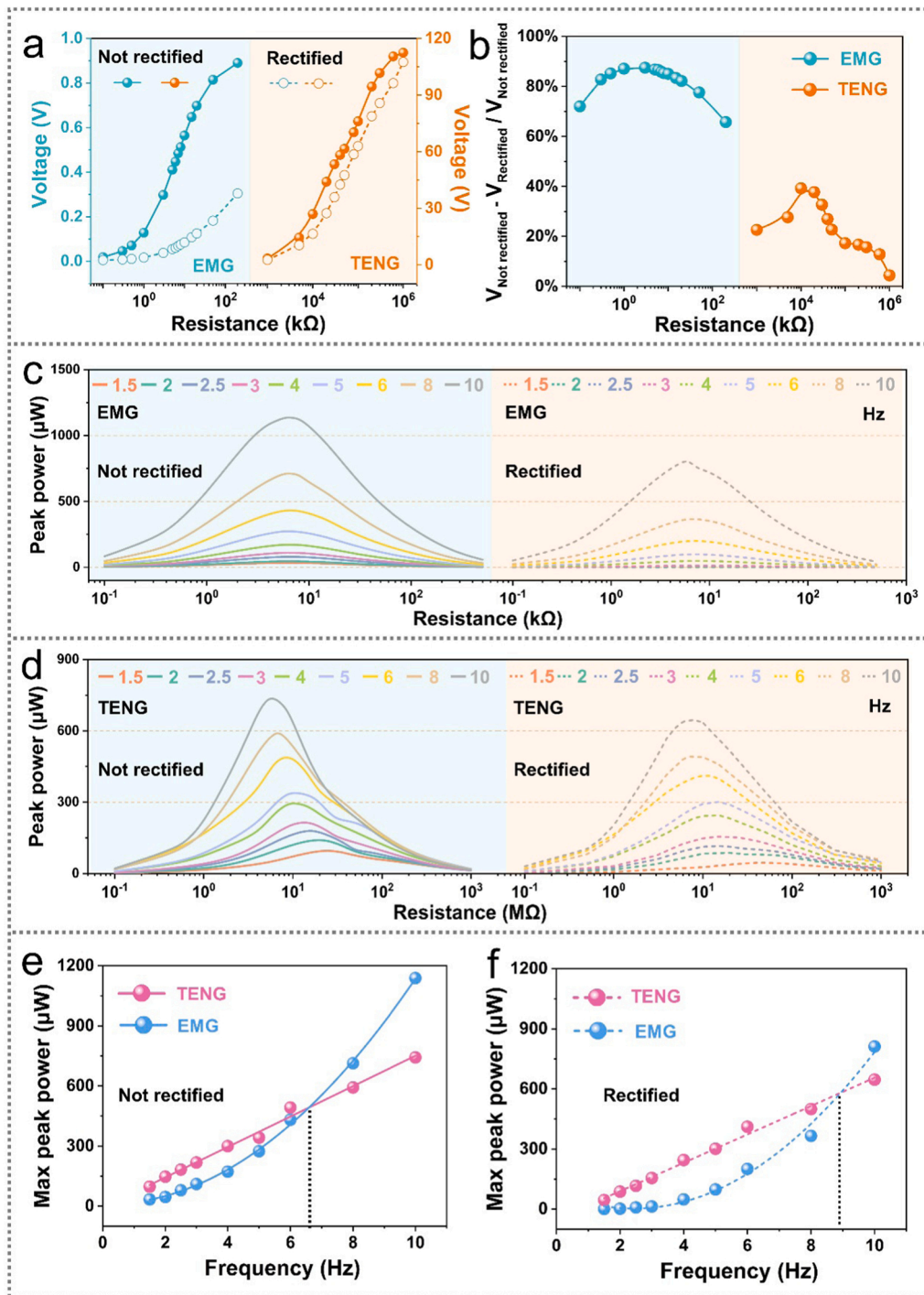


Fig. 2. Loss of peak power at different frequencies for EMG and TENG after rectification. (a–b) Output voltage (a) and voltage loss rate (b) before and after rectification for EMG and TENG with various load resistors connected at 1.5 Hz. (c–d) Peak power of EMG (c) and TENG (d) at different frequencies before and after rectification. (e–f) Maximum peak power for both generators without rectification (e) and after rectification (f).

and V_{OC} is the open circuit voltage. Since the surface size of TENG, the speed of motion, the thickness of the dielectric material and all other parameters are defined values, the open circuit voltage and internal resistance of TENG are a fixed value. Moreover, the internal resistance of diodes in the rectifier bridge is generally tens of ohms to hundreds of ohms, and the internal resistance of EMG is 6.7k ohms, and the internal resistance of TENG reaches megohm level. Therefore, the resistance of the rectifier bridge is basically negligible compared to the internal resistance of the two generators even if the rectifier consists of different types of diodes.

From Eq. (1) we can analyze that since R_R is a fixed value, the magnitude of $\eta_{V_{loss}}$ is determined by the resistance of $(R_L + r)$. For EMG, $(R_L + r)$ ranges from a few thousand ohms, while that of TENG reaches several megohms. Therefore the $\eta_{V_{loss}}$ of TENG is smaller than that of EMG due to the larger internal resistance of TENG. Fig. 2b shows the experimental results of the voltage loss rate at 1.5 Hz and illustrates the smaller $\eta_{V_{loss}}$ of TENG than EMG, which is consistent with the theoretical analysis. Nevertheless, the $\eta_{V_{loss}}$ is increased first and decreased gradually with the enhancement of R_L , meaning that the $\eta_{V_{loss}}$ at a small load resistance is lower than that of theoretical value. It may be related to the

effect of the noise signal on the real voltage signal with a small resistor connected at the rectification circuit. Fig. S2 (Supporting information) shows that the noise signal from the environment results in a larger voltage than real value with a minimum resistor connected, thus causing the value of $V_{Not\ rectified} - V_{Rectified}$ to be smaller than the theoretical one. Moreover, Fig. S3 (Supporting information) demonstrates the voltage loss of EMG and TENG at other frequencies and the results are consistent with the above conclusions.

Since the rectification circuit leads to the loss of output voltage, it can also impose an impact on output power theoretically. The peak power and average power of the load resistance can be described as [41]:

$$P_{peak} = \left(\frac{V_{OC, peak}}{R_L + r} \right)^2 \bullet R_L = \frac{V_{L, peak}^2}{R_L} \quad (2)$$

$$P_{average} = \frac{\int_0^T V_L^2 dt}{R_L T} = \left(\frac{\overline{V_{OC}}}{R_L + r} \right)^2 \bullet R_L \quad (3)$$

where $V_{OC, peak}$ and $\overline{V_{OC}}$ are the maximum and average values of the open circuit voltage, respectively. V_L is the voltage of the load, and T and t are the period and time, respectively. Fig. 2c and Fig. 2d illustrate the peak power of EMG and TENG before and after rectification at different frequencies. The peak power of EMG improves with increasing frequency before rectification, and the best matching resistance measured at different frequencies is kept around 6–7 k Ω , which is basically equal to the coil internal resistance, as shown in Fig. 2c. As EMG does not have the property of internal capacitance, its internal resistance is equal to the copper coil resistance, so it is not affected by the motion frequency, and the optimal impedance matching point of the EMG is basically the same at different frequencies. Moreover, the variation characteristics of the results at the rectification circuit are consistent with the above and the peak power is significantly diminished after rectification. For TENG, the peak power varies in same way as EMG with the increase of frequency and it decays slightly after rectification, and the best matching resistance of TENG decreases as the frequency increases, as shown in Fig. 2d. Since TENG has the property of internal capacitance, the faster the generator moves, the smaller the impedance of TENG will be, as reported previously [46]. Therefore, the matching impedance of TENG decreases gradually with increasing frequency. The above results indicate that the rectification circuit causes a greater attenuation of peak power to EMG than to TENG.

To further evaluate the effect of rectifier on the output performance of EMG and TENG at different frequencies, we first compare the maximum peak power, average output power, and output energy versus frequency of both generators theoretically. When R_L is equal to r , the maximum peak power and the maximum average power can be obtained from Eq. (2) and Eq. (3). According to previous reports, the maximum open-circuit voltage of EMG are linearly proportional to frequency [42], as can be described as $V_{OC, peak}^{EMG} \propto f$. Since the internal resistance of the EMG is a constant, the maximum peak power of the EMG versus f can be deduced from Eq. (2) as $P_{peak, max}^{EMG} \propto f^2$.

In addition, the relationship between the average power and f can be derived theoretically. For EMG in contact separation mode, the open circuit voltage and the absolute value of V_{OC} can be denoted as:

$$V_{OC}^{EMG} = -N \frac{d\Phi}{dt} = -NS \frac{dB}{dt} \quad (4)$$

$$\left| \overline{V_{OC}^{EMG}} \right| = \left| \frac{\int_0^T V_{OC}^{EMG} dt}{T} \right| = \left| \frac{-NS \int_0^T \frac{dB}{dt} dt}{T} \right| = 2NBSf \quad (5)$$

where N and S are the number of turns and area of the coil, Φ is the magnetic flux through the coil, and B is the magnetic field. The factor 2

is attributed to the fact that the flux through the coil changes twice (from maximum to zero and from zero to maximum) in one cycle. Combining Eq. (3) and Eq. (5), the maximum average power of EMG is derived:

$$P_{average, max}^{EMG} = \frac{(2NBSf)^2}{4r} = \frac{(NBSf)^2}{r} \quad (6)$$

In the case of TENG, V_{OC} is independent of f [41,42] while the impedance of TENG is inversely proportional to f [46]. Combining the above analysis and Eq. (2), the relationship between the maximum peak power of TENG and f can be formulated as $P_{peak, max}^{TENG} \propto f$.

Besides, previous simulations of TENG shows that the optimal average power of TENG is roughly proportional to the frequency with the matching resistor connected [46–48], as given below (D is a constant):

$$P_{average, max}^{TENG} \propto f \quad \text{or} \quad \log_{10} P_{average, max}^{TENG} = \log_{10} f + D \quad (\text{approximately}) \quad (7)$$

Furthermore, the optimum output energy is achieved while R_L equals to r and it versus f can be analyzed by referring to the relationship between energy and average power, and the output energy can be expressed as:

$$E = P_{average} T = \frac{\int_0^T V_L^2 dt}{R_L T} \quad T = \frac{\int_0^T V_L^2 dt}{R_L} \quad (8)$$

it reveals that the output energy is proportional to the average power. The result indicates that the output energy of EMG is proportional to the square of f while that of TENG is proportional to f .

Based on the analysis above, a series of experiments have been carried out and the results of the maximum peak power of EMG and TENG at various frequencies before rectification are present in Fig. 2e. It illustrates that the fitting curve of the maximum peak power of EMG shows a quadratic function relationship with frequency while linear relationship with TENG, which is consistent with the theoretical derivation. The maximum peak power of TENG is superior to that of EMG at frequencies not exceeding 6 Hz while inferior to EMG on the contrary. As for the maximum peak power after rectification, the frequency range where the power of TENG is greater than that of EMG is extended to 9 Hz, as demonstrated in Fig. 2f, which can be attributed to the larger power depletion of EMG and little attenuation of TENG. Fig. S4 (Supporting information) displays the maximum peak power loss rate after rectification for both generators, which is calculated by the ratio of the lost power caused by rectification to the maximum peak power before rectification, showing that the loss of EMG is much more severe than that of TENG.

Fig. 3a indicates that the average power density of TENG is smaller than that of EMG when not rectified, and they are extremely close to each other at low frequencies. Besides, the fitting curve of average power density of TENG and EMG is linear and quadratic relationship with frequency, respectively, which is consistent with the theoretical analysis. After rectification, owing to the more severe power loss of EMG compared to TENG, the average power density of EMG is smaller than that of TENG at frequencies not exceeding 5 Hz, as shown in Fig. 3b. Fig. S5 (Supporting information) illustrates the average power loss per cubic centimeter of EMG and TENG, indicating that the loss of TENG is always lower than that of EMG. Fig. 3c and Fig. 3d demonstrate the output energy of both generators in 2 s before and after rectification with frequency varies from 1.5 Hz to 10 Hz. The results reveal that the effect of rectification on output energy is basically the same as the effect on average power. At frequency not exceeding 5 Hz, the energy density of TENG after rectification is superior to that of EMG, which is improved than the result without rectification. In addition, the detailed energy integration curves are exhibited in Fig. S6 (Supporting information) and the value of energy loss per cubic centimeter for TENG and EMG at different frequencies are shown in Fig. S7 (Supporting information). The reasons for more severe power and energy losses of EMG than that of

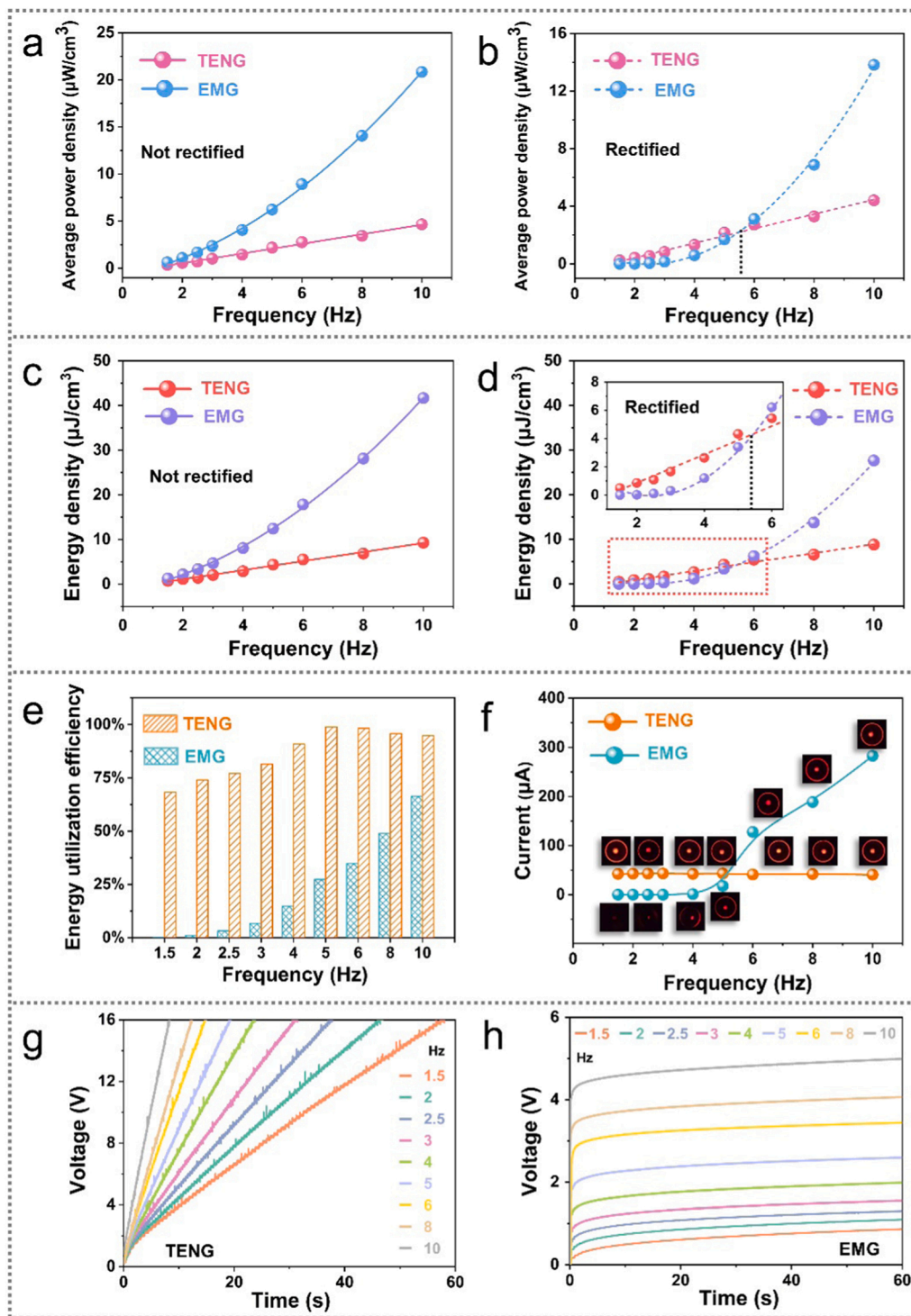


Fig. 3. Loss of energy at different frequencies for EMG and TENG after rectification and practical applications for both generators. (a–b) Comparison of the average power density of EMG and TENG at different frequencies without rectification (a) and after rectification (b). (c–d) Comparison of the total output energy for 2 s of EMG and TENG per cm^3 at different frequencies before (c) and after (d) rectification. (e) Energy utilization efficiency of the both generators with the rectifier bridge act as the energy management unit. (f) The current through the LED at different frequencies and the corresponding LED luminous photographs as both generators power the LED directly. Each set of photos was taken at frequencies of 1.5 Hz, 2.5 Hz, 4 Hz, 5 Hz, 6 Hz, 8 Hz, and 10 Hz, respectively. (g–h) Voltage of charging $1\mu\text{f}$ capacitor at different frequencies of TENG (g) and EMG (h).

TENG are described in detail in the [Supplementary Note 1](#). Fig. 3e demonstrates the energy utilization efficiency of both generators with the rectifier act as the energy management unit, which characterizes the ratio of the maximum output energy before and after rectification. The result demonstrates that the energy utilization efficiency of EMG is inferior to that of TENG at various frequencies, and it is merely 0.26 % for EMG while can up to 68.27 % for TENG at 1.5 Hz. At a frequency of 5 Hz, the energy utilization efficiency of TENG reach the maximum of 98.84 %, and then it stabilizes and reduces slightly as the frequency increases. TENG achieves the maximum energy utilization efficiency at 5 Hz may be also related to the inadequate contact between the two

tribo-materials of TENG at high frequency. According to Eq. (8), the output energy is proportional to the average power, and [Supplementary Note 2](#) described that when the frequency is excessive (> 5 Hz), the average power loss rate of TENG gradually increases, so the loss rate of output energy also gradually increases, therefore the energy utilization of TENG no longer increases at a frequency greater than 5 Hz. Therefore, some measures we can take to achieve complete contact between the two tribo-layers to further reduce the energy loss during rectification, such as physical or chemical treatment of the material surface, choosing a softer friction material, or selection of a liquid material as the tribo-layer.

Moreover, the maximum utilization efficiency of EMG is up to 66.36 %, but it is much less than that of TENG of 98.84 %. The different energy loss of TENG and EMG is mainly caused by the different degree of drop in output voltage of the load resistor after accessing the rectifier bridge. The output voltage of the load resistor will change after the rectifier bridge is connected, and the voltage change rate of TENG is much smaller than that of EMG. Since the output energy is proportional to the square of output voltage (as shown in Eq. (8)), the output energy of TENG after rectification is reduced only a little due to a slight drop in voltage, which leads to a low energy losses and thus a high energy utilization efficiency of 98.84 %. In contrast, the rectified EMG has a larger voltage loss rate, as shown in Fig. 2b, resulting in a roughly larger energy loss and a low energy utilization efficiency of 66.36 %.

In practical applications, the generators can directly drive the LED, and the current through the LED and the corresponding LED luminous photos at different frequencies are shown in Fig. 3f. At frequencies not exceeding 5 Hz, the LED driven by TENG is brighter and the current is larger than that of EMG. As the frequency exceeds 5 Hz, the EMG-driven LEDs have larger current, and the brightness of LEDs is comparable to that driven by TENG to the naked eye. Fig. 3g and Fig. 3h displays the curves of charging 1 μF capacitor by rectified TENG and EMG, respectively, and it illustrates that the saturation voltage of the capacitor charged by TENG is always larger than that of the capacitor charged by

EMG at various frequencies.

In order to verify the accuracy of the conclusion that the effect of rectification on the losses of the output performance on EMG is more severe than the effect on TENG, we measured the output power and energy of EMGs with various turns and various wire diameters. The resistance of the load connected in the circuit always matches the internal resistance of the coil, and the resistance of coils are presented in Section 2. Fig. 4a and Fig. 4b demonstrate the open-circuit voltage and short-circuit current for EMG with different wire diameters and same turns (13,000 turns) at various frequencies, indicating that they both show a good linear relationship with frequency basically. Moreover, the open-circuit voltage diminishes while the short-circuit current grows gradually as the wire diameter increases, and the change in voltage can be attributed to the variation in the number of effective turns. With the magnetic flux changing from the maximum (minimum) to the minimum (maximum), the effective displacement between the magnet and the coil is a constant, and the effective number of turns corresponding to a thicker wire is smaller than that of a thinner one at the same displacement, thus the corresponding open circuit voltage is smaller. In addition, a thicker coil corresponds to a smaller resistance, which leads to larger short-circuit currents. Fig. 4c compares the maximum peak power of EMGs with different wire diameters before and after rectification. Before rectification, the maximum peak power grows gradually first as the wire

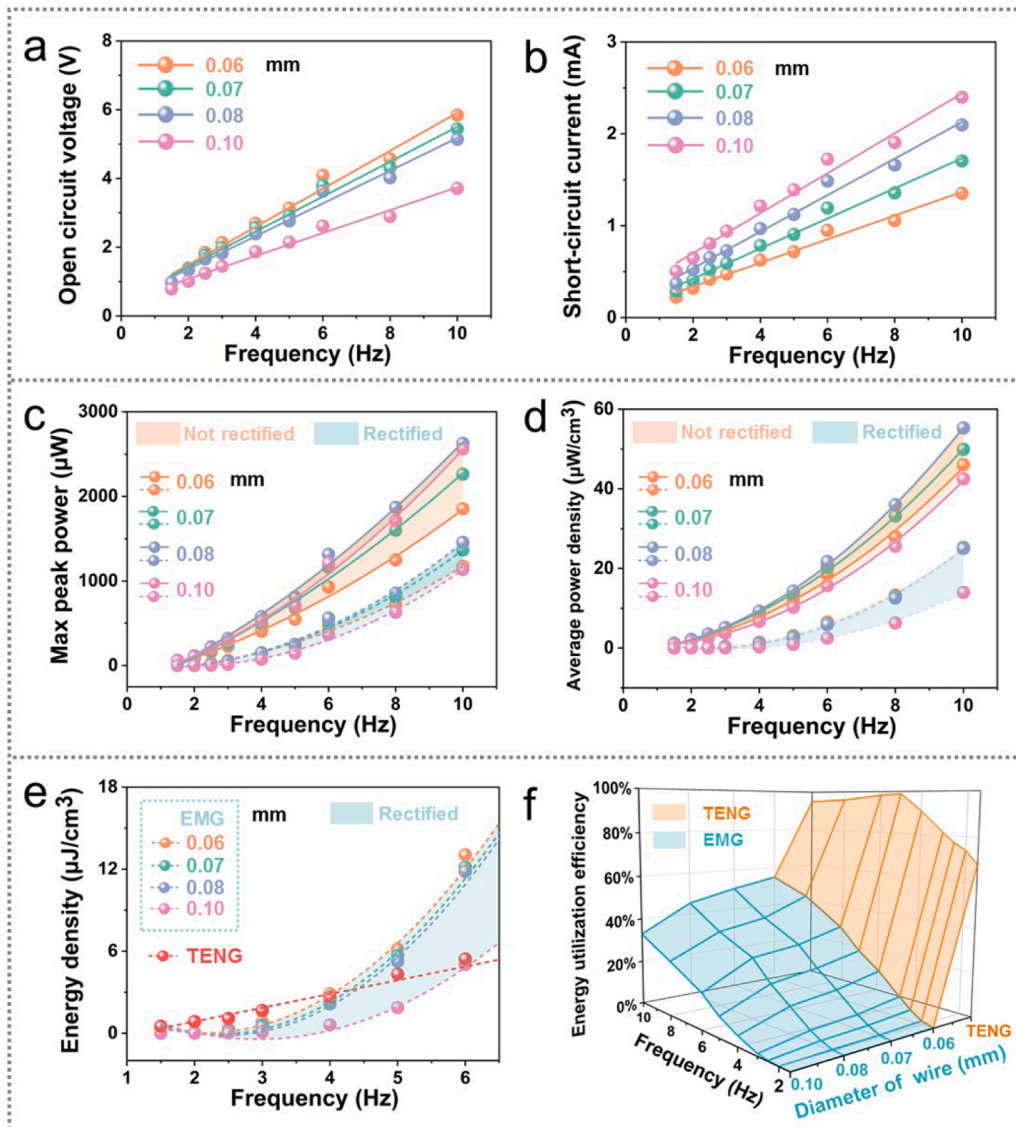


Fig. 4. Output performance of EMG fabricated with different wire diameters of coils before and after rectification at different frequencies. (a–b) Open-circuit voltage (a) and short-circuit current (b) for EMGs with different wire diameters at various frequencies. (c–d) Maximum peak power (c) and average power density (d) before and after rectification for EMGs with different wire diameters. (e) Comparison of energy density after rectification of TENG and EMG with different wire diameters. (f) Energy utilization efficiency of TENG and EMG with different wire diameters.

diameter increases to 0.08 mm and then decreases slightly as the wire diameter up to 0.1 mm, and the decline of power may be also related to the decrease in the effective number of turns of the coil. After rectification, the maximum peak powers of all different coils are reduced. In addition, Fig. 4d shows the average power densities of EMGs with different wire diameters before and after rectification, and the results are essentially the same as the changing law of the maximum peak power. Fig. 4e compares the energy density of TENG and EMGs with different wire diameters after rectification and shows that the energy density of TENG is greater than that of EMG at frequencies less than 4 Hz and is inferior to EMG at frequencies above 4 Hz. Nevertheless, the energy density of TENG is always smaller than EMGs with different wire diameters without rectification, as exhibited in Fig. S8 (Supporting information). The above results reveal that the rectification causes much more energy loss to EMG than to TENG, especially at low frequency. Fig. 4f displays the energy utilization efficiency of TENG and above EMGs and that of EMG grows gradually as the wire diameter gets thinner and frequency gets larger, and the maximum value reaches 54.83 % at a wire diameter of 0.06 mm and frequency of 10 Hz, whereas all utilization efficiency are smaller than TENG at the same frequency.

In addition, a series of experiments on the output performance of EMGs with various turns and same wire diameter of 0.05 mm were

carried out. Fig. 5a and Fig. 5b indicates that the open-circuit voltage improves and the short-circuit current falls respectively as the number of turns increases, and the decline in short-circuit current can be attributed to the larger internal resistance of coil with more turns. Furthermore, the maximum peak power rises gradually with the increase of turns before rectification and it shows the same pattern after rectification, as shown in Fig. 5c. Fig. 5d demonstrates that the average power density increases basically with the increasing of turns, and there is a slight decrease at turns of 25,000 T, which is due to the current drop caused by the excessive resistance. Fig. 5e compares the energy density of TENG and the EMG with various turns after rectification and illustrates that the energy density of TENG is more advantageous than that of EMGs with various turns while the frequency is roughly below 2.5 Hz. Meanwhile, the energy density of TENG and EMGs with various turns before rectification is shown in Fig. S9 (Supporting information). Fig. 5f compares the energy utilization efficiency of TENG and above EMGs. Similarly, the energy utilization efficiency of EMG increases gradually with the coil turns and frequency grows, and reaching a maximum value of 71.73 % at a turn of 25,000 T and frequency of 10 Hz, yet all the values are inferior to that of TENG at the same frequency. From the above results we can conclude that reducing the wire diameter of the coil and increasing the number of turns can improve the energy utilization

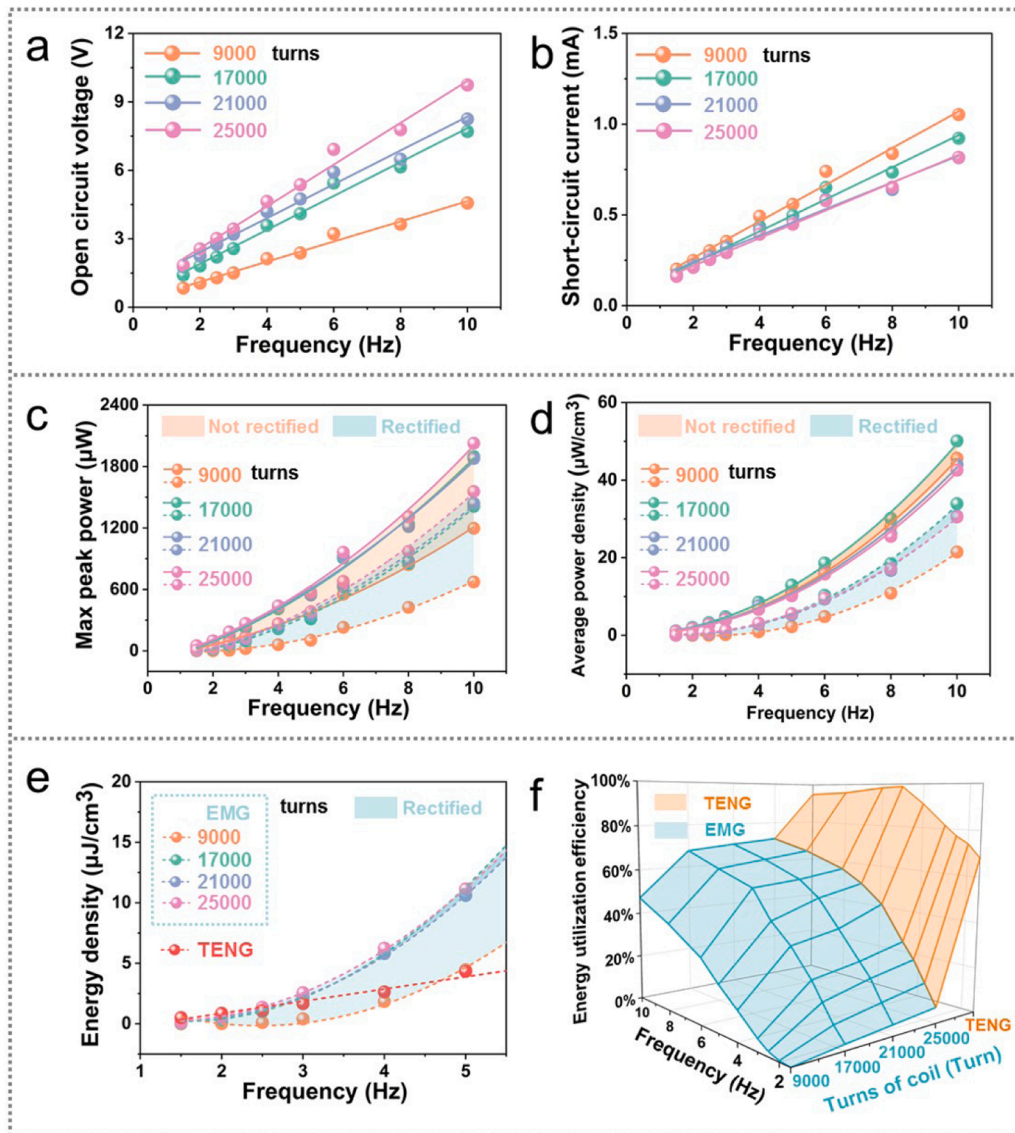


Fig. 5. Output performance of EMG fabricated with different turns of coils before and after rectification at different frequencies. (a–b) Open-circuit voltage (a) and short-circuit current (b) for EMGs with different turns at various frequencies. (c–d) Maximum peak power (c) and average power density (d) before and after rectification for EMGs with different turns. (e) Comparison of energy density after rectification of TENG and EMG with different turns. (f) Energy utilization efficiency of TENG and EMG with different turns.

efficiency of EMG, so the energy loss of EMG after rectification can be further reduced by optimizing the coil parameters.

4. Conclusion

In summary, we compared the loss of output performance of TENG and EMG in contact-separation mode at different frequencies after rectification. The results illustrate that the voltage loss rate after rectification for EMG is more serious than that of TENG, and it is rather severe at low frequencies for EMG compared to that of TENG, leading to a more significant loss of the output power and energy for EMG. The maximum peak power of TENG is higher than that of EMG at low frequencies before rectification, and the frequency range in which TENG outperforms EMG is further expanded after rectification due to the more severe peak power loss of EMG than that of TENG. Besides, the average power loss rate decreases roughly with increasing frequency and the loss rate of TENG is consistently lower than that of EMG at same frequency, and it is especially obvious at low frequencies, reaching a maximum of 31.73 % for TENG and 99.74 % for EMG at a low frequency of 1.5 Hz. Moreover, the energy utilization efficiency of TENG is always larger than that of EMG at various frequency, with a minimum of 68.27 % and a maximum of 98.84 % for TENG, while the corresponding values for EMG are only 0.26 % and 66.36 %, and this contrasting characteristics is verified in EMG with different number of turns and different wire diameters. This work reveals the superiority of TENG compared to EMG in terms of a low loss of power and energy after rectification, and provides an important guidance for the study of the applications of DC-TENG.

CRediT authorship contribution statement

Ya Yang conceived the idea and guided the project. Chaosheng Hu fabricated the devices and performed measurements. Chaosheng Hu, Ya Yang and Zhong Lin Wang discussed experimental results, drew figures, and prepared the manuscript. All authors contributed to data analysis and commented on the manuscript.

Declaration of Competing Interest

The authors declare that they have no known competing financial interests or personal relationships that could have appeared to influence the work reported in this paper.

Data Availability

Data will be made available on request.

Acknowledgments

This work was supported by the National Key R & D Project from Minister of Science and Technology in China (No. 2021YFA1201604), the National Natural Science Foundation of China (No. 52072041), and the University of Chinese Academy of Sciences (Grant no. Y8540XX2D2).

Appendix A. Supporting information

Supplementary data associated with this article can be found in the online version at [doi:10.1016/j.nanoen.2022.107760](https://doi.org/10.1016/j.nanoen.2022.107760).

References

- [1] C. Wu, T.W. Kima, S. Sung, J.H. Park, F. Li, *Nano Energy* 44 (2018) 279–287.
- [2] Y. Chen, Y. Kuang, D. Shi, M. Hou, X. Chen, L. Jiang, J. Gao, L. Zhang, Y. He, C.-P. Wong, *Nano Energy* 73 (2020), 104765.
- [3] Q. Zeng, Y. Wu, Q. Tang, W. Liu, J. Wu, Y. Zhang, G. Yin, H. Yang, S. Yuan, D. Tan, C. Hu, X. Wang, *Nano Energy* 70 (2020), 104524.

- [4] S. Wang, X. Mu, Y. Yang, C. Sun, A.Y. Gu, Z.L. Wang, *Adv. Mater.* 27 (2015) 240–248.
- [5] B. Chen, Y. Yang, Z.L. Wang, *Adv. Energy Mater.* 8 (2018) 1702649.
- [6] X. Liu, P. Cui, J. Wang, W. Shang, S. Zhang, J. Guo, G. Gu, B. Zhang, G. Cheng, Z. Du, *Nanotechnology* 32 (2021), 075401.
- [7] T. Bhatta, P. Maharjan, M. Salauddin, M.T. Rahman, S.M.S. Rana, J.Y. Park, *Adv. Funct. Mater.* 30 (2020) 2003276.
- [8] S. Li, D. Liu, Z. Zhao, L. Zhou, X. Yin, X. Li, Y. Gao, C. Zhang, Q. Zhang, J. Wang, Z. L. Wang, *ACS Nano* 14 (2020) 2475–2482.
- [9] Y. Jiang, K. Dong, X. Li, J. An, D. Wu, X. Peng, J. Yi, C. Ning, R. Cheng, P. Yu, Z. L. Wang, *Adv. Funct. Mater.* 31 (2020) 2005584.
- [10] D. Liu, B. Chen, J. An, C. Li, G. Liu, J. Shao, W. Tang, C. Zhang, Z.L. Wang, *Nano Energy* 73 (2020), 104819.
- [11] S. Zhang, J. Guo, L. Liu, H. Ruan, C. Kong, X. Yuan, B. Zhang, G. Gu, P. Cui, G. Cheng, Z. Du, *Nano Energy* 91 (2022), 106660.
- [12] J. Huang, X. Fu, G. Liu, S. Xu, X. Li, C. Zhang, L. Jiang, *Nano Energy* 62 (2019) 638–644.
- [13] Q. Shi, T. He, C. Lee, *Nano Energy* 57 (2019) 851–871.
- [14] T. Jiang, H. Gao, J. An, P. Lu, Y. Feng, X. Liang, W. Zhong, Z.L. Wang, *Adv. Energy Mater.* 10 (2020), 200064.
- [15] L. Gao, S. Lu, W. Xie, X. Chen, L. Wu, T. Wang, A. Wang, C. Yue, D. Tong, W. Lei, H. Yu, X. He, X. Mu, Z.L. Wang, Y. Yang, *Nano Energy* 72 (2020), 104684.
- [16] Z.L. Wang, T. Jiang, L. Xu, *Nano Energy* 39 (2017) 9–23.
- [17] W. Zhang, G. Gu, H. Qin, S. Li, W. Shang, T. Wang, B. Zhang, P. Cui, J. Guo, F. Yang, G. Cheng, Z. Du, *Nano Energy* 77 (2020), 105108.
- [18] W. Zhang, G. Gu, W. Shang, H. Luo, T. Wang, B. Zhang, P. Cui, J. Guo, F. Yang, G. Cheng, Z. Du, *Nano Energy* 86 (2021), 106056.
- [19] X. Chen, L. Gao, J. Chen, S. Lu, H. Zhou, T. Wang, A. Wang, Z. Zhang, S. Guo, X. Mu, Z.L. Wang, Y. Yang, *Nano Energy* 69 (2020), 104440.
- [20] C. Ye, K. Dong, J. An, J. Yi, X. Peng, C. Ning, Z.L. Wang, *ACS Energy Lett.* 6 (2021) 1443–1452.
- [21] X. Wang, S. Wang, Y. Yang, Z.L. Wang, *ACS Nano* 9 (2015) 4553–4562.
- [22] T. Quan, Y. Yang, *Nano Res.* 9 (2016) 2226–2233.
- [23] T. Quan, Y. Wu, Y. Yang, *Nano Res.* 8 (2015) 3272–3280.
- [24] X. Wang, Y. Yang, *Nano Energy* 32 (2017) 36–41.
- [25] X. Zhong, Y. Yang, X. Wang, Z.L. Wang, *Nano Energy* 13 (2015) 771–780.
- [26] Y. Chen, Y. Cheng, Y. Jie, X. Cao, N. Wang, Z.L. Wang, *Energy Environ. Sci.* 12 (2019) 2678–2684.
- [27] Z. Yi, D. Liu, L. Zhou, S. Li, Z. Zhao, X. Li, Z.L. Wang, J. Wang, *Nano Energy* 84 (2021), 105864.
- [28] D. Liu, L. Zhou, Z.L. Wang, J. Wang, *iScience* 24 (2021), 102018.
- [29] J. Wang, Z. Wu, L. Pan, R. Gao, B. Zhang, L. Yang, H. Guo, R. Liao, Z.L. Wang, *ACS Nano* 13 (2019) 2587–2598.
- [30] R. Cheng, K. Dong, P. Chen, C. Ning, X. Peng, Y. Zhang, D. Liu, Z.L. Wang, *Energy Environ. Sci.* 14 (2021) 2460–2471.
- [31] Y. Song, N. Wang, Y. Wang, R. Zhang, H. Olin, Y. Yang, *Adv. Energy Mater.* 10 (2020) 2002756.
- [32] J. Wang, Y. Li, Z. Xie, Y. Xu, J. Zhou, T. Cheng, H. Zhao, Z.L. Wang, *Adv. Energy Mater.* 10 (2020) 1904227.
- [33] C. Shan, W. Liu, Z. Wang, X. Pu, W. He, Q. Tang, S. Fu, G. Li, L. Long, H. Guo, J. Sun, A. Liu, C. Hu, *Energy Environ. Sci.* 14 (2021) 5395–5405.
- [34] H.J. Yoon, M. Kang, W. Seung, S.S. Kwak, J. Kim, H.T. Kim, S.W. Kim, *Adv. Energy Mater.* 10 (2020) 2000730.
- [35] Y. Gao, D. Liu, L. Zhou, S. Li, Z. Zhao, X. Yin, S. Chen, Z.L. Wang, J. Wang, *Nano Energy* 85 (2021), 106014.
- [36] L. Zhou, D. Liu, S. Li, Z. Zhao, C. Zhang, X. Yin, L. Liu, S. Cui, Z.L. Wang, J. Wang, *Adv. Energy Mater.* 10 (2020) 2000965.
- [37] Z. Zhao, Y. Dai, D. Liu, L. Zhou, S. Li, Z.L. Wang, J. Wang, *Nat. Commun.* 11 (2020) 6186.
- [38] Z. Zhang, D. Jiang, J. Zhao, G. Liu, T. Bu, C. Zhang, Z.L. Wang, *Adv. Energy Mater.* 10 (2020) 1903713.
- [39] X. Liang, T. Jiang, G. Liu, T. Xiao, L. Xu, W. Li, F. Xi, C. Zhang, Z.L. Wang, *Adv. Funct. Mater.* 29 (2019) 1807241.
- [40] C. Zhang, W. Tang, C. Han, F. Fan, Z.L. Wang, *Adv. Mater.* 26 (2014) 3580–3591.
- [41] Y. Zi, H. Guo, Z. Wen, M.H. Yeh, C. Hu, Z.L. Wang, *ACS Nano* 10 (2016) 4797–4805.
- [42] J. Zhao, G. Zhen, G. Liu, T. Bu, W. Liu, X. Fu, P. Zhang, C. Zhang, Z.L. Wang, *Nano Energy* 61 (2019) 111–118.
- [43] F. Gao, Z. Zhang, Q. Liao, G. Zhang, Z. Kang, X. Zhao, X. Xun, Z. Zhao, L. Xu, L. Xue, Y. Zhang, *Adv. Energy Mater.* 9 (2019) 1901881.
- [44] H.L. Wang, Z.H. Guo, G. Zhu, X. Pu, Z.L. Wang, *ACS Nano* 15 (2021) 7513–7521.
- [45] Z. You, S. Wang, Z. Li, Y. Zou, T. Lu, F. Wang, B. Hu, X. Wang, L. Li, W. Fang, Y. Liu, *Nano Energy* 91 (2022), 106667.
- [46] S. Niu, S. Wang, L. Lin, Y. Liu, Y.S. Zhou, Y. Hu, Z.L. Wang, *Energy Environ. Sci.* 6 (2013) 3576–3583.
- [47] S. Niu, Z.L. Wang, *Nano Energy* 14 (2015) 161–192.
- [48] S. Niu, Y. Liu, X. Chen, S. Wang, Y.S. Zhou, L. Lin, Y. Xie, Z.L. Wang, *Nano Energy* 12 (2015) 760–774.



Chaosheng Hu is currently a doctoral candidate in the research group of Prof. Ya Yang at Beijing Institute of Nanoenergy and Nanosystems, Chinese Academy of Sciences (CAS). His research interests are focused on triboelectric nanogenerator and ferroelectric material.



Ya Yang received his Ph.D. in Materials Science and Engineering from University of Science and Technology Beijing, China. He is currently a professor at Beijing Institute of Nanoenergy and Nanosystems, Chinese Academy of Sciences, China. He has developed ferroelectric materials-based various new hybridized and multi-effects coupled devices, opening up the new principles of the device design and coupled effects, and the new approaches of improving output performances of energy-related devices. His main research interests focus on the field of ferroelectric materials for energy conversion, self-powered sensing, and some new physical effects. Details can be found at: <http://www.researcherid.com/rid/A-7219-2016>.



Zhong Lin (ZL) Wang received his Ph.D. from Arizona State University in physics. He now is the Hightower Chair in Materials Science and Engineering, Regents' Professor, Engineering Distinguished Professor and Director, Center for Nanostructure Characterization, at Georgia Tech. Dr. Wang has made original and innovative contributions to the synthesis, discovery, characterization and understanding of fundamental physical properties of oxide nanobelts and nanowires, as well as applications of nanowires in energy sciences, electronics, optoelectronics and biological science. His discovery and breakthroughs in developing nanogenerators established the principle and technological road map for harvesting mechanical energy from environment and biological systems for powering personal electronics. His research on self-powered nanosystems has inspired the worldwide effort in academia and industry for studying energy for micro-nano-systems, which is now a distinct disciplinary in energy research and future sensor networks. He coined and pioneered the field of piezotronics and piezophotonics by introducing piezoelectric potential gated charge transport process in fabricating new electronic and optoelectronic devices. Details can be found at: <http://www.nanoscience.gatech.edu>.